Aeroacoustic Instability in Rockets

Gary A. Flandro*
University of Tennessee Space Institute, Tullahoma, Tennessee 37388
and
Joseph Majdalani†
Marquette University, Milwaukee, Wisconsin 53233

Current solid-propellant rocket instability calculations (e.g., Standard Stability Prediction Program) account only for the evolution of acoustic energy with time. However, the acoustic component represents only part of the total unsteady system energy; additional kinetic energy resides in the shear waves that naturally accompany the acoustic oscillations. Because most solid-rocket motor combustion chamber configurations support gas oscillations parallel to the propellant grain, an acoustic representation of the flow does not satisfy physically correct boundary conditions. It is necessary to incorporate corrections to the acoustic wave structure arising from generation of vorticity at the chamber boundaries. Modifications of the classical acoustic stability analysis have been proposed that partially correct this defect by incorporating energy source/sink terms arising from rotational flow effects. One of these is Culick's flow-turning stability integral; related terms that are not found in the acoustic stability algorithm appear. A more complete representation of the linearized motor aeroacoustics is utilized to determine the growth or decay of the system energy with rotational flow effects accounted for already. Significant changes in the motor energy gain/loss balance result; these help to explain experimental findings that are not accounted for in the present acoustic stability assessment methodology.

Nomenclature

$A_b^{(r)}$	=	admittance of burning surfaces
$A_N^{(r)}$	=	nozzle admittance
$A_S^{(r)}$	=	admittance of nonburning surfaces
a_0	=	mean speed of sound
E	=	time-averaged oscillatory system energy
E_m^2	=	normalization constant for mode m
e	=	oscillatory energy density
$\boldsymbol{e}_r, \boldsymbol{e}_\theta, \boldsymbol{e}_z$	=	unit vectors in r, θ, and z directions
k_m	=	wave number for axial mode m, $m\pi R/L$
L	=	chamber length
M_b	=	reference Mach number at burning surface
m	=	mode number
$\boldsymbol{n}$	=	outward-pointing unit normal vector
P_0	=	mean chamber pressure
p	=	oscillatory pressure
R	=	chamber radius
r	=	radial position
S	=	Strouhal number, k_m/M_b
t	=	time
U_r, U_z	=	mean flow velocity components
$\boldsymbol{u}$	=	oscillatory velocity vector
y	=	radial distance from the wall, $1-r$
z	=	axial position
α	=	growth rate (dimensional, s^{-1})
γ	=	ratio of specific heats
δ	=	inverse square root of the acoustic Reynolds number, $\sqrt{(\nu/a_0 R)}$
ε	=	wave amplitude
ν	=	kinematic viscosity, μ/ρ
ρ	=	density
$\phi(r)$	=	function defined in Eq. (13)
$\psi(r)$	=	exponential argument; Eq. (11)
Ω	=	mean vorticity amplitude
ω	=	unsteady vorticity amplitude

Subscripts

b	=	combustion zone
m	=	mode number

Superscripts

$(r), (i)$	=	real/imaginary or cosine/sine parts
$*$	=	dimensional quantity
$\sim$	=	vortical (rotational) part
$\wedge$	=	acoustic (irrotational) part

I. Introduction

CULICK'S papers on combustion instability[1-5] published in the early 1970s are the foundation for stability prediction methods now in use.[6,7] His method is based on three crucial assumptions: 1) small-amplitude pressure fluctuations superimposed on a low-speed mean flow; 2) thin, chemically reacting surface layer with mass addition; and 3) oscillatory flowfield represented by chamber acoustic modes.

The first assumption allows linearization of the governing equations both in the wave amplitude and the surface Mach number of the mean injected flow. The second causes all surface reaction effects, including combustion, to collapse to simple acoustic admittance boundary conditions imposed at the chamber surfaces. The last assumption oversimplifies the oscillatory gas dynamics by suppressing all unsteady rotational flow effects; the acoustic representation is strictly irrotational. Concern for this omission was partially addressed by Culick in a paper in which he introduced his well-known rotational mean flow model.[2] Stability calculations based on this improved mean flow representation produced no significant changes in the system stability characteristics. On this basis, it has since been generally assumed that all vorticity (rotational flow effects), including the unsteady part, has negligible influence on combustion instability growth rate calculations.

Considerable progress has been made in the last decade in understanding both the precise source of the vorticity and the resulting

changes in the oscillatory flowfield. Approximate analytical,[8−16] numerical,[17−22] and experimental investigations[23−26] have demonstrated that rotational flow effects play an important role in the unsteady gas motions in solid-rocket motors. Much effort has been directed to constructing the required corrections to the acoustic model. This has culminated in a comprehensive picture of the unsteady motions that agrees with experimental measurements,[8−10] as well as numerical simulations.[11]

These models were used in carrying out three-dimensional system stability calculations[8,9] in a first attempt to account for rotational flow effects by correcting the acoustic instability algorithm. In this process one discovers the origin, and the three-dimensional form, of the classical flow-turning correction; related terms appear that are not accounted for in the Standard Stability Prediction Program algorithm. In particular, a rotational correction term is identified that cancels the flow-turning energy loss in a full-length cylindrical grain. However, all of these results must now be questioned because they are founded on an incomplete representation of the system energy balance.

Culick's stability estimation procedure is based on calculating the exponential growth (or decay) of an irrotational acoustic wave; the results are equivalent to energy balance models used earlier by Cantrell and Hart.[27] In all of these calculations the system energy is represented by the classical Kirchoff (acoustic) energy density. Consequently, it does not represent the full unsteady field, including both acoustic and rotational flow effects. Kinetic energy carried by the vorticity waves is ignored. It will be demonstrated in this paper that the actual average unsteady energy contained in the system at a given time is about 25% larger than the acoustic energy alone. Furthermore, representation of the energy sources and sinks that determine the stability characteristics of the motor chamber must also be modified. Attempts to correct the acoustic growth rate model by retention of rotational flow source terms only[8,9] preclude a full representation of the effects of vorticity generation and coupling.

In fact, there is a convincing body of evidence pointing to the existence of other aeroacoustic coupling mechanisms that are not incorporated in the current acoustic-stability theory. For example, the so-called parietal or surface vortex shedding (PVS) has been identified some years ago as a source of instability that eludes classic theory.[28] The corresponding phenomenon was first detected by numerical simulations of 1:5 subscale models of the French Ariane V booster.[29−32] This P230 Moteur à Propergol Solide (MPS) was known to exhibit large amplitude oscillations.[33] This new type of instability was especially important in long, segmented rocket motors such as the Japanese H-II vehicle,[34] the Titan 34D solid rocket motor (SRM),[35] the Titan IV SRM/SRMU (upgrade),[36−39] the shuttle rocket booster (SRB),[40] and other motors with length-to-portradius ratios ranging from 15 to 25.

To compensate for the inability of classic theory[3,5,41−48] to explain the large pressure oscillations driven by so-called "crawling" vortices,[29] a number of studies have been carried out with the aim of improving our basic understanding of the suspected mechanism.[28] Credit should be given, in that regard, to Vuillot, Avalon, Casalis, Griffond, Lupoglazoff, Traineau, Dupays, Pineau, Tissier, Ugurtas, and coworkers who have employed experimental,[28,49−52] numerical,[53−59] and theoretical avenues[60−63] to elucidate the origin of PVS coupling. In Refs. 60–63 Casalis, Avalon, Pineau, and Griffond have based their recent theoretical study on linear instability theory introduced in 1969 by Varapaev and Yagodkin.[64] Their efforts have provided an alternate source of instability whose omission in classic analyses has led them to associate some of the unforeseen experimental and numerical instabilities to the hydrodynamic evolution and inception of mean flow turbulence.[60,61]

At the conclusion of these studies,[30−32,50−52] speculations that resonance-like pressure amplifications were caused only by vortex shedding at annular restrictors or inhibitor rings were laid to rest when similarly intense vorticity-generated oscillations were observed in unsegmented rocket motors. As noted by Ugurtas et al.,[65] two-dimensional compressible flow simulations of the Navier–Stokes equations by Lupoglazoff and Vuillot[29−31] have confirmed the measurements acquired from subscale firings; as such, the

collection of all available data has pointed out to the existence of a powerful vorticity-driven coupling irrespective of whether inhibitor rings or other surface anomalies are present.[29−31]

The studies just reviewed demonstrate that current motor stability assessments based on irrotational flow effects alone cannot properly represent the observed system behavior. The main objective of this paper is the construction of a more complete model for the stability of rocket motor flowfields that accounts for interactions that are lost in the irrotational (acoustic unsteady flow) assumption. Stability terms must be identified that will establish the correct energy pathways between the rotational and the irrotational parts of the gas oscillations. This is best accomplished by applying the energy balance approach because this method enhances the physical understanding of the many gas dynamic interactions involved in the problem.

Considerable work is needed to make these improvements. The outcome is a stability algorithm that accounts for both acoustic and vortical flow interactions. Although no attempt is made in this paper to explore all possible unsteady flowfield configurations, stability terms are deduced that will allow such flow effects to be included in the stability assessment. For example, whereas turbulence effects and surface vortices (as in the parietal vortex shedding mechanism) are not addressed directly, the terms in the stability balance in which detailed representations of these additional vortical flow effects enter the problem will be identified.

Significant differences between these new results and those currently utilized for motor stability computations are demonstrated. The new model is tested by applying it to several solid-propellant rocket motor configurations to demonstrate important scaling and geometrical effects. A new energy source term is identified that represents at least one way in which unexplained instabilities in large solid propellant booster motors arise. This energy source, arising from production of unsteady vorticity at the propellant burning surface, can be comparable in size to the key combustion pressure coupling itself. It might also be related to velocity coupling effects, which cannot be fully represented in the context of irrotational acoustic instability theory. This same term, when evaluated using vortex shedding flow solutions, yields an improved description of this energy source.

Despite major changes in the mathematical formulation, it is not necessary to discard the current linear stability estimation methodology; required modifications are readily accomplished by adding the new stability integrals to those already in place in the current stability codes. It is important to note that all of the original terms identified in the earlier irrotational models are recovered in the more complete results described in this paper.

II. Unsteady Flow Analysis

The goal of this section is the construction of an improved model of the unsteady flowfield in a rocket chamber that realistically accounts for vortical (rotational) as well as acoustical (irrotational) effects. In particular, close attention is paid to properly satisfying the correct boundary conditions on all chamber boundaries including both inert and reactive surfaces.

The validity of the stability calculations depends critically on a sufficiently detailed and physically correct representation of the unsteady velocity field. The assumption of an irrotational unsteady flow as used in most stability calculations must be discarded. The analytical methods and notation employed here closely follow earlier papers.[8−10] Dimensionless variables are the same as those used in the classical combustion instability analyses: velocities are normalized by dividing by the average sound speed, and pressure is normalized by dividing by the product of the mean chamber pressure and the specific heat ratio γ. Other thermodynamic properties are made dimensionless by dividing them by their mean chamber reference values. Lengths are referenced to the chamber radius R. Figure 1 illustrates the geometry and coordinate systems to be employed in the analysis.

The analysis starts by assuming small-amplitude unsteady perturbations on a mean flow described by the vector $M_b \boldsymbol{U}$. In this paper Culick's mean flow model[2] for a cylindrical burning port

$$\boldsymbol{U} = U_r \boldsymbol{e}_r + U_z \boldsymbol{e}_z = -r^{-1}\sin x \boldsymbol{e}_r + \pi z \cos x \boldsymbol{e}_z \qquad (1)$$
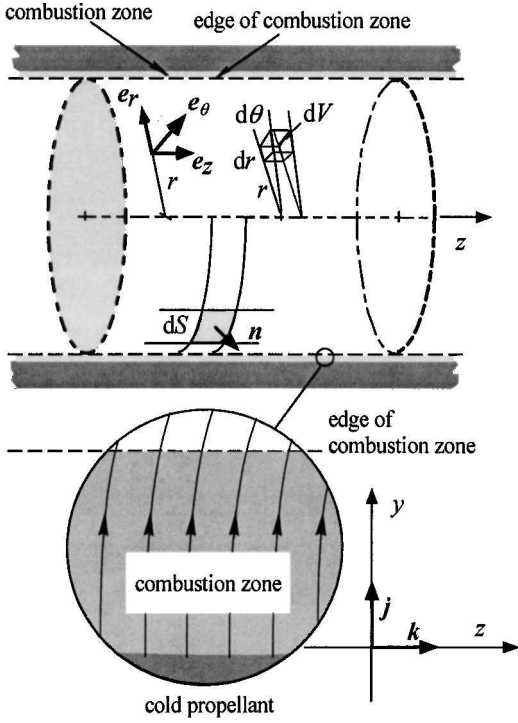
Fig. 1   Motor geometry and coordinate system used.

will be used. Note that the combination

$$x \equiv \tfrac{1}{2}\pi r^2 \qquad (2)$$

appears frequently in the analysis.

Isentropic conditions are assumed, but viscous forces, both shear and dilatational, are retained. The linearized continuity and momentum equations then become

$$\frac{\partial \rho^{(1)}}{\partial t} + \nabla \cdot \boldsymbol{u}^{(1)} = -M_b \boldsymbol{U} \cdot \nabla \rho^{(1)} \qquad (3)$$

$$\frac{\partial \boldsymbol{u}^{(1)}}{\partial t} + \nabla p^{(1)} = M_b \left\{ -\nabla \left[\boldsymbol{U} \cdot \boldsymbol{u}^{(1)} \right] + \boldsymbol{u}^{(1)} \times \nabla \times \boldsymbol{U} + \boldsymbol{U} \times \nabla \times \boldsymbol{u}^{(1)} \right\}$$

$$+ \delta^2 \left\{ \left(2 + \frac{\lambda}{\mu} \right) \nabla \left[\nabla \cdot \boldsymbol{u}^{(1)} \right] - \nabla \times \nabla \times \boldsymbol{u}^{(1)} \right\} \qquad (4)$$

This dimensionless set of equations is the starting point for all preceding combustion instability models. The superscript (1) denotes the first-order terms in a perturbation parameter ε proportional to the amplitude of the unsteady pressure fluctuation. A second small parameter, the mean flow Mach number at the burning surface M_b, is also employed in the linearization process; only terms to the first order in M_b are retained as in the classical combustion instability analyses. The relative size of the viscous forces is set by the parameter δ^2, which is the inverse of the acoustic Reynolds number based on the chamber radius R. Viscous terms are usually dropped, but are retained here for completeness by assuming that $\delta^2 = \mathcal{O}(M_b)$.

The main variables will be represented as combinations of irrotational and rotational components:

$$\begin{cases} p^{(1)} = \hat{p} + \tilde{p} \\ \rho^{(1)} = \hat{p} \\ \boldsymbol{u}^{(1)} = \hat{\boldsymbol{u}} + \tilde{\boldsymbol{u}} \end{cases} \qquad (5)$$

The acoustic field is irrotational ($\nabla \times \hat{\boldsymbol{u}} = 0$), and the superimposed vortical component is incompressible ($\nabla \cdot \tilde{\boldsymbol{u}} = 0$). Because of the assumption of constant entropy, the density and the thermodynamic (acoustic) pressure are interchangeable as indicated in Eq. (5). The density in the continuity equation is routinely replaced in the classical analysis by the pressure variable. The reader is cautioned that

care must be taken in interpreting the unsteady pressure $p^{(1)}$. If it appears in the continuity equation, this parameter will then represent a density fluctuation. This distinction is not important if the flow is irrotational, but it is vitally important when rotational effects are to be incorporated.

If irrotational flow is assumed, Eqs. (3) and (4) yield the usual acoustic wave solutions. For axial motions in a rocket chamber, the solution is the standing plane wave

$$\hat{p} = e^{-ikt} \cos(k_m z) + \mathcal{O}(M_b) \qquad (6)$$

$$\hat{\boldsymbol{u}} = i e^{-ikt} \sin(k_m z) \boldsymbol{e}_z + \mathcal{O}(M_b) \qquad (7)$$

For axial modes satisfaction of closed-end boundary conditions requires that

$$k_m = m\pi R/L \qquad (8)$$

As Eqs. (6) and (7) indicate, there exist corrections to the acoustic field of the order of the mean Mach number. These were described in Ref. 8, but are not required in the stability calculations. Only the first-order velocity and pressure (in M_b) are needed in evaluating the stability integrals.

It is immediately apparent that Eq. (7) cannot satisfy physically correct boundary conditions either at the edge of the combustion zone or on inert side walls. The axial velocity component must approach zero at the wall to satisfy the no-slip condition. Thus the production of axial acoustic oscillations gives rise to corrections that must come from the rotational flow effects. Flandro solved Eqs. (3) and (4) for the vortical (rotational, incompressible) field by two different methods. The inviscid case was treated in Ref. 8; a more complete analysis was presented in Ref. 9, in which viscous shear wave damping was included. Another improvement in the latter was the introduction of an equivalent closed-form solution in place of the infinite series used in Ref. 8. Additional improvements were made in Ref. 10, in which turbulent mean flow corrections were introduced. For clarity, we will display only the laminar results for the simplest motor geometry and acoustic mode structure, namely, a cylindrical port with axial oscillations; other geometries and transverse modes of oscillation can be handled similarly. Other investigators such as Majdalani and Roh[16] have verified the basic results to be used here by quite different analytical approaches and by direct fluid dynamics computations.[11–19]

For rotational pressure and velocity corrections that must accompany the assumed acoustic solution of Eqs. (6) and (7), one finds

$$\tilde{p} = i M_b e^{-ikt} \sin(2x) e^{(\phi + i\psi)} \left(\tfrac{1}{2}\pi z \right) \sin[\sin(x) k_m z] + \mathcal{O}(M_b^2) \qquad (9)$$

$$\tilde{\boldsymbol{u}} = i C e^{-ikt} r U_r e^{(\phi + i\psi)} \sin[\sin(x) k_m z] \boldsymbol{e}_z + \mathcal{O}(M_b) \qquad (10)$$

An undetermined complex constant C is shown in Eq. (10). In the earlier work this constant was evaluated by assuming that, for a thin combustion layer, the physical boundary at the solid surface and the edge of the combustion zone are nearly coincident.[8–10] Then if one applies the no-slip condition to the composite unsteady axial velocity [$\boldsymbol{u}^{(1)} = \hat{\boldsymbol{u}} + \tilde{\boldsymbol{u}}$] at the edge of the combustion zone, one finds that $C = 1$. This result has been questioned because the actual solid surface lies within a region of nonuniformity, the combustion zone (Brown, R.S., private communication, Tullahoma, Tennessee, Sept. 2000). It is a straightforward process to show that the original value is correct; the calculation is too lengthy to display here. This is done by constructing a two-dimensional model for the combustion zone including all gas phase effects. The axial momentum equation in the flame zone is solved numerically to account for the gradients in temperature and density caused by combustion. The resulting inner solution is then matched asymptotically to the outer solution expressed by Eq. (10). Standard methods of singular perturbation theory apply. The simplest approach is to determine solutions in an intermediate region in which both the outer and inner representations are valid. Then the matching is readily accomplished. The outcome confirms that the original result, $C = 1$, is correct unless the oscillation frequency is very high. In that case the rotational flow

effects become entirely buried within the combustion zone, and the outer solution collapses to the simple plane wave acoustic model.

Flandro[9] derived these expressions directly from Eqs. (3) and (4) without recourse to the splitting theorem applied in earlier papers. Critics have not understood that splitting Eqs. (3) and (4) into acoustical and vortical parts (following the method of Chu and Kovásznay[66] and Morse and Ingard[67]) is a simplifying, but not a necessary, step in arriving at the solutions displayed (Brown, private communication). Another misunderstanding centers on the pressure correction, $\tilde{p}$, sometimes called the pseudopressure. It is important to understand that this was not simply set to zero by assumption in the earlier works. Careful solution of the momentum equation (4) shows that it is an additional correction of the order of the mean Mach number; the result is shown in Eq. (9). Corrections of similar size appear in the irrotational (acoustic) pressure solution Eq. (6). Although $\tilde{p}$ constitutes a negligible contribution to the overall pressure, its incorporation is helpful in the acoustic stability calculations for reasons that will be described later. It is also necessary to point out that the pseudopressure must not be inserted in the continuity (3), as part of the density variable as suggested by Brown in his 2000 private communication.

The complex exponential factor $\exp(\phi + i\psi)$ in the solution exhibited in Eq. (10) suggests that the vortical motion can be interpreted as a damped traveling shear wave. Both ϕ and ψ are functions only of radial position. The imaginary part of the exponential argument, namely,

$$\psi(r) = -[k_m/(\pi M_b)]\ln\tan\left(\tfrac{1}{2}x\right) \qquad (11)$$

sets the wavelength and spatial frequency of the shear wave. For later use note that the derivative of ψ with respect to the radius is simply

$$\frac{d\psi}{dr} = \frac{k_m}{M_b U_r} \qquad (12)$$

This is proportional to the reciprocal of the radial mean flow velocity. The real part of the argument $\phi(r)$ is given by

$$\phi(r) = \frac{\xi}{\pi^2}\left[1 - \frac{1}{\sin(x)} - x\frac{\cos(x)}{\sin^2(x)} + I(x) - I\left(\frac{1}{2}\pi\right)\right]$$

$$\xi \equiv \frac{k_m^2\delta^2}{M_b^3} = \frac{S^2\delta^2}{M_b}, \qquad S \equiv \frac{k_m}{M_b} \qquad (13)$$

$$I(x) = x + \frac{1}{18}x^3 + \frac{7}{1800}x^5 + \frac{31}{105,840}x^7 + \cdots \qquad (14)$$

where ξ is a parameter of $\mathcal{O}(1)$ that reflects the relative importance of the viscous damping; its physical description and verification are detailed by Majdalani and Roh.[16] Note that the damping of the shear wave in the radial direction increases quadratically as the frequency of the acoustic oscillation increases. Similarly, the wavelength of the shear wave decreases as frequency increases. For the fundamental acoustic mode and the lowest order harmonics, the shear wave might fill the entire chamber; for high-order acoustic modes the shear oscillations become confined to a thin acoustic boundary layer, which can lie entirely within the combustion zone.[13]

The composite axial velocity solution found by superimposing Eqs. (7) and (10) has been shown[8–10,12] to agree quite closely with the experimental findings of Refs. 12, 25, 26, and 68. Figures 2 and 3 show comparisons of the oscillation amplitude and phase angle from the theory just discussed superimposed on some of Brown's earlier cold flow work.[24,69] It is important to understand that no curve fitting has been used here; the differences between the experimental and theoretical results arise both from unavoidable experimental errors (orientation and positioning of the hot film sensor, data reduction, etc.) and from the assumption set used in the analysis. Nevertheless,
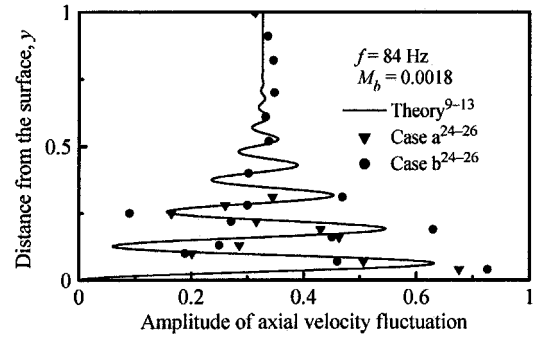

Fig. 2   Comparison of theoretical and experimental amplitudes of unsteady axial velocities. Here $S = 51.3m$, $z^*/L = 0.106$, $M_b = 0.0018$, $L/R = 34$, $k_m = 0.0924m$, $\xi = 0.539m^2$, **and** $m = 1$. **Triangles and circles correspond to experimental data acquired with a pressure wave amplitude of a) 0.0005 and b) 0.0039.**
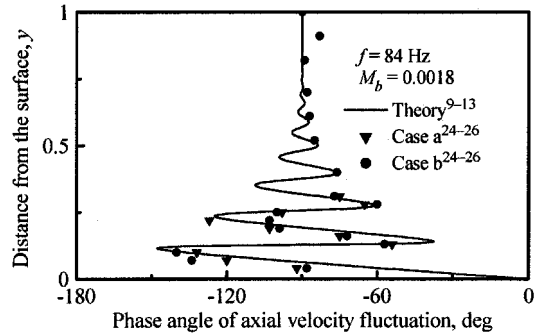

Fig. 3   Comparison of theoretical and experimental phase angles (degrees).

adequate agreement is shown. Because nitrogen was the working fluid at measured temperature and pressure, all parameters characterizing the flowfield are well known.

Numerical solutions based on the full Navier–Stokes representation of the unsteady field also indicate excellent agreement with the theory reviewed here. Furthermore, other analytical methods based on Wentzel, Kramers, and Brillouin (WKB) and multiple-scale theories have been applied by Majdalani and Van Moorhem.[70] Theirs have demonstrated, based on the principle of least singularity, the existence of nonlinear scales underlying the physics of the problem.[71] In addition to providing a rigorous mathematical treatment that does not require guesswork, their approach has led to the exact form of the characteristic length scales as function of Culick's mean flow solution. Particularly, their solutions have yielded results that are virtually indistinguishable from those displayed here.[11–16]

In previous analyses of the rocket motor rotational flowfield, special attention was given to the radial component of velocity.[8,9,11] This was done because, in classical instability theory, the main source of acoustic energy is the radial velocity fluctuation produced by interaction of the pressure wave with the combustion processes and heat transfer in the burning zone. It was shown in Refs. 8 and 9 that, in addition to the radial acoustic velocity, there appears a rotational correction that does not vanish at the edge of the combustion zone. The presence of this additional unsteady radial velocity component implies that, by analogy to pressure coupling, there is an additional source of unsteady mass flux at the combustion zone interface. For want of better terminology, this was called the rotational flow correction as first displayed in Eq. (89) of Ref. 8. The new term, which does not appear in any previous analysis, has given rise to considerable controversy.

By way of providing a precise description of the source of the rotational flow correction, a detailed physical interpretation, and a full resolution of the controversy, will appear in the next section of this paper. The answers are found by means of a careful derivation of the system stability energy balance. It is not necessary to calculate the vortical radial velocity correction in determining the system stability. The surface acoustic admittance function will be utilized

in the standard fashion to represent the pressure coupling of the oscillatory flow with the combustion processes. Then experimental measurements (usually secured with a T-burner or similar device) of the surface response can be utilized as in the accepted methodology for accounting for this important source of oscillatory energy.

Earlier attempts to incorporate vortical flow corrections in the stability calculations were based on the idea that one must restore rotational source terms which were dropped in the classical analyses. For example, Brown, et al.[24] had suggested that retention of the rotational convective acceleration term $U \times \nabla \times u^{(1)}$ on the right side of Eq. (4) might have important stability implications. This term was first evaluated by Flandro,[8,9] who showed that this term yields a damping effect that is indistinguishable from the classical flow-turning loss. Additional terms that cannot be found in the standard stability computations appear in this analysis. One of these, the rotational flow correction, has led to much debate because it exactly cancels the flow-turning effect in some chamber configurations. Brown's assertion that the rotational flow correction is just another way to represent flow turning can be quite readily refuted. In fact, all misunderstandings are resolved when a consistent energy method is used to deduce motor stability characteristics. The flaw in the earlier approach is that it represented the system by a model that accounts for growth or decay of the acoustic energy alone. Simply retaining the rotational convective source terms[24] in the perturbed wave equation, following Culick's method, does not address this important defect.

To describe the evolution of the oscillatory flow in a rocket motor correctly, all unsteady energy must be accounted for first. The method used here follows the known energy balance approach described by Kirchoff[72] and used extensively in rocket stability calculations by Cantrell and Hart[27] and Hart and coworkers.[41−43] It is now necessary to account for the entire kinetic energy fluctuation. To accomplish this, multiply the continuity equation (3) by the acoustic pressure (or density) and add this to the momentum equation (4), multiplied by the composite unsteady velocity vector,

$$u^{(1)} = \hat{u} + \tilde{u} \qquad (15)$$

This operation constitutes the main departure from the preceding approach. Isolating the terms differentiated with respect to time and retaining only those terms that are linear in the Mach number M_b, one finds

$$\frac{\partial}{\partial t}\left[\frac{1}{2}\hat{p}^2 + \frac{1}{2}u^{(1)} \cdot u^{(1)}\right] = -\left[\hat{p}\nabla \cdot \hat{u} + u^{(1)} \cdot \nabla(\hat{p} + \tilde{p})\right]$$

$$- M_b\left\{\frac{1}{2}U \cdot \nabla\hat{p}^2 + u^{(1)} \cdot \nabla\left[U \cdot u^{(1)}\right]\right.$$

$$\left. - u^{(1)} \cdot \left[u^{(1)} \times \nabla \times U + U \times \nabla \times \tilde{u}\right]\right\}$$

$$+ \delta^2 u^{(1)} \cdot \left[\left(2 + \frac{\lambda}{\mu}\right)\nabla(\nabla \cdot \hat{u}) - \nabla \times \nabla \times \tilde{u}\right] \qquad (16)$$

If the full unsteady velocity vector $u^{(1)}$ were to be replaced at this stage by the acoustic part $\hat{u}$, then the final result of the stability calculation would be exactly that described in earlier papers.[8,9] If all rotational terms on the right of Eq. (16) were also to be removed by assuming that $\tilde{u} = 0$, then the classical three-dimensional stability result would be reproduced. Assumptions such as those just described are motivated mainly by a desire to keep the analysis simple. However, as we shall now demonstrate much physical substance is lost in such simplifications. We choose not to follow the traditional approach here—most rotational effects are retained as Eq. (16) shows; the kinetic energy per unit mass on the left-hand side reflects all laminar unsteady motions in the chamber. Parietal-vortex shedding and turbulent corrections will require special attention and future refinements; discussions of turbulent flow effects are found in the numerical studies by Flandro et al.,[10] Roh et al.,[18] Yang and Roh,[19] Apte and Yang,[73] Beddini and Roberts,[74,75] and Vuillot and coworkers.[57,58] So that the analysis is not overly complicated,

effects of solid particles in the flow are not displayed either; required modifications are to be incorporated later as needed.

Following the standard approach,[72] one defines the oscillatory energy density

$$e = \frac{1}{2}\left[\hat{p}^2 + u^{(1)} \cdot u^{(1)}\right] \qquad (17)$$

and the time-averaged oscillatory energy residing in the chamber at any instant as

$$E = \iiint_V \langle e \rangle \, dV = \frac{1}{2}\iiint_V \left\langle \hat{p}^2 + u^{(1)} \cdot u^{(1)}\right\rangle dV \qquad (18)$$

where triangular brackets denote the time average of the enclosed function. Then from Eq. (16) it is clear that the evolution of the system energy is controlled by

$$\frac{\partial E}{\partial t} = \iiint_V \left\langle \overbrace{-\nabla \cdot (\hat{p}\hat{u}) - \frac{1}{2}M_b(U \cdot \nabla\hat{p}^2) - M_b[\hat{u} \cdot \nabla(U \cdot \hat{u})]}^{\text{irrotational}} \right.$$

$$+ \delta_d^2\hat{u} \cdot \nabla(\nabla \cdot \hat{u}) + M_b[\hat{u} \cdot (\hat{u} \times \Omega) + \hat{u} \cdot (U \times \omega)]$$

$$\overbrace{- \tilde{u} \cdot \nabla\hat{p} - M_b\begin{bmatrix}\tilde{u} \cdot \nabla(U \cdot \hat{u}) + \hat{u} \cdot \nabla(U \cdot \tilde{u}) + \tilde{u} \cdot \nabla(U \cdot \tilde{u}) \\ -\tilde{u} \cdot (U \times \omega) - \tilde{u} \cdot (\tilde{u} \times \Omega)\end{bmatrix}}^{\text{rotational}}$$

$$+ \delta_d^2\tilde{u} \cdot \nabla(\nabla \cdot \hat{u}) - \delta^2[\hat{u} \cdot (\nabla \times \omega) + \tilde{u} \cdot (\nabla \times \omega)]$$

$$\left. - \hat{u} \cdot \nabla\tilde{p} - \tilde{u} \cdot \nabla\tilde{p}\right\rangle dV \qquad (19)$$

where the irrotational and rotational contributions to the energy rate of change have been partitioned for clarity. The last two "irrotational" terms are in reality caused by rotational effects. They are placed with the irrotational terms to conform to Culick's methodology.[2,47] The last two "rotational" terms are caused by the pseudopressure, a quantity that has often been ignored in previous studies. The mean and unsteady vorticity vectors are represented in Eq. (19) by $\Omega = \nabla \times U$ and $\omega = \nabla \times \tilde{u}$, respectively.

The dilatational viscous term is simplified by defining

$$\delta_d^2 \equiv \delta^2(2 + \lambda/\mu) \qquad (20)$$

where λ is the second coefficient of viscosity. Several terms cancel. For example,

$$-\hat{u} \cdot (\tilde{u} \times \Omega) - \tilde{u} \cdot (\hat{u} \times \Omega) = 0 \qquad (21)$$

Further simplifications can be made. For example, several terms can be expressed as integrals over the surface bounding the control volume. It is first necessary to review the protocol needed in evaluating the stability integrals.

The terms on the right-hand side of Eq. (19) control the rate at which the system energy changes. From this information one can estimate the growth or decay rate for a given motor configuration. The complex wave number (or frequency) k in the assumed exponential time dependence is written as

$$k = k_m + (\omega_m + i\alpha_m) + \mathcal{O}(M_b^2) \qquad (22)$$

In the multidimensional case m can consist of three mode integers. We will restrict the evaluation to axial modes for clarity; then a single integer m identifies the mode being investigated. More complex modes can be handled in a similar way. The result for a simple plane wave axial mode is shown in Eq. (8). The dimensionless corrections $\omega_m + i\alpha_m$ are of the order of the mean flow Mach number. In the conventional energy-balance procedure the frequency correction ω_m is not evaluated. For simplicity, we follow this approach. The frequency correction is implicitly accounted for in the wave number k_m.

Because quadratic combinations of the variables appear, it is first necessary to take the real parts of the pressure and velocities to be inserted in the equations. Thus one writes

$$\hat{p} = \hat{p}_m \exp(\alpha_m t)\cos(k_m t) \tag{23}$$

$$\hat{\boldsymbol{u}} = \hat{\boldsymbol{u}}_m \exp(\alpha_m t)\sin(k_m t) \tag{24}$$

$$\tilde{\boldsymbol{u}} = \exp(\alpha_m t)\left[\tilde{\boldsymbol{u}}_m^{(r)}\cos(k_m t) + \tilde{\boldsymbol{u}}_m^{(i)}\sin(k_m t)\right] \tag{25}$$

where superscripts (r) and (i) refer to the cosine and sine multipliers stemming from complex-to-real conversion of real and imaginary parts. This notation is necessary because the rotational velocity vector contains the spatial exponential term $\exp(\phi + i\psi)$. Inserting these expressions into Eq. (17) yields the time-averaged energy density

$$\langle e \rangle = \tfrac{1}{4}\exp(2\alpha_m t)\Big[\overbrace{\hat{p}_m^2 + \hat{\boldsymbol{u}}_m \cdot \hat{\boldsymbol{u}}_m}^{\text{irrotational}}$$

$$+ \underbrace{2\hat{\boldsymbol{u}}_m \cdot \tilde{\boldsymbol{u}}_m^{(i)} + \tilde{\boldsymbol{u}}_m^{(r)} \cdot \tilde{\boldsymbol{u}}_m^{(r)} + \tilde{\boldsymbol{u}}_m^{(i)} \cdot \tilde{\boldsymbol{u}}_m^{(i)}}_{\text{rotational}}\Big] \tag{26}$$

which has been partitioned to emphasize the new terms. This result should be compared to the classical expression for the energy density, which consists of only the first two terms in Eq. (26). The additional three terms represent the kinetic energy residing in the unsteady vorticity. Inserting these expressions into Eq. (18), carrying out the time averaging, and differentiating with respect to time, one finds

$$\frac{\partial E}{\partial t} = \alpha_m \exp(2\alpha_m t) E_m^2 \tag{27}$$

where the energy normalization function

$$E_m^2 = \frac{1}{2}\iiint_V \Big[(\hat{p}_m')^2 + \hat{\boldsymbol{u}}_m \cdot \hat{\boldsymbol{u}}_m + 2\hat{\boldsymbol{u}}_m \cdot \tilde{\boldsymbol{u}}_m^{(i)}$$

$$+ \tilde{\boldsymbol{u}}_m^{(r)} \cdot \tilde{\boldsymbol{u}}_m^{(r)} + \tilde{\boldsymbol{u}}_m^{(i)} \cdot \tilde{\boldsymbol{u}}_m^{(i)}\Big]\, dV \tag{28}$$

is expressed here by the same symbol used in earlier stability analyses. It is written as a squared quantity to indicate that it is positive definite.

It is interesting to compare values from Eq. (28) to those found in earlier computations. The mode shapes are needed for this purpose. Equations (6), (7), and (10) give the required information for the assumed axial oscillations to zeroth order in M_b:

$$\hat{p}_m = \cos(k_m z) \tag{29}$$

$$\hat{\boldsymbol{u}}_m = \sin(k_m z)\boldsymbol{e}_z \tag{30}$$

$$\tilde{\boldsymbol{u}}_m^{(r)} = \sin(x)\exp(\phi)\sin(\psi)\sin[\sin(x)k_m z]\boldsymbol{e}_z \tag{31}$$

$$\tilde{\boldsymbol{u}}_m^{(i)} = -\sin(x)\exp(\phi)\cos(\psi)\sin[\sin(x)k_m z]\boldsymbol{e}_z \tag{32}$$

The acoustic pressure and velocity mode shapes are related by

$$\hat{\boldsymbol{u}}_m = -\nabla\hat{p}_m / k_m \tag{33}$$

for later use. Figure 4 shows the results of integration of the kinetic energy terms in Eq. (28) across the chamber from the centerline to the wall at a given axial location. Note that the term involving the cross product of the acoustic and vortical parts does not contribute to the integrated result because it oscillates in the radial direction and is zero at the upper limit. However, the rotational correction shows a net value, which is half of the integrated acoustic energy density. Clearly, the rotational effects represent a significant change in the system energy.

When the entire volume integral of Eq. (28) is carried out for the axial mode case, using Eqs. (29–32) one finds that

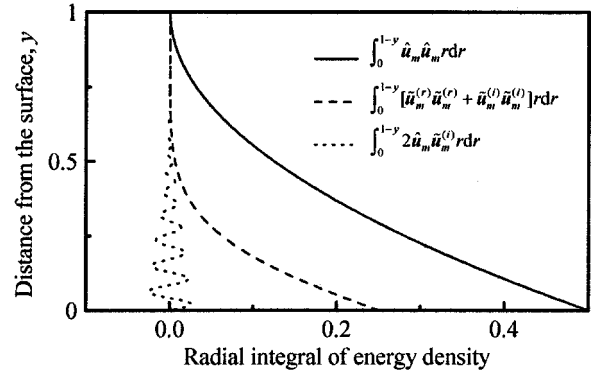$$E_m^2 = \tfrac{5}{8}\pi L/R \tag{34}$$

Fig. 4   Radial integration of the kinetic energy density components.

which is 25% larger than the conventional acoustic value for longitudinal oscillations. However, the most important changes in the growth rate α_m appear in the integral terms on the right-hand side of Eq. (19). We must now attend to this important part of the stability analysis.

A.   Growth Rate Calculations

In estimating the system growth rate for a given mode of oscillation, it can be seen that it consists of the linear superposition of 15 volume integrals as shown in Eq. (19). The simplest procedure is to consider each of these (or selected groups) to be evaluated individually. One can then represent the net growth rate as a linear sum of gains and losses as

$$\alpha_m = \alpha_1 + \alpha_2 + \alpha_3 + \cdots = \sum_{i=1}^{N}\alpha_i \tag{35}$$

in the usual fashion. The dimensionless values of the several terms are given in the following paragraphs. The reader is reminded that, in order to compute the corresponding dimensional values, it is necessary to multiply by a_0/R, the inverse of the characteristic time used in the formulation. Then the growth rates are obtained in the familiar units of rad/s (s^{-1}).

B.   Irrotational Growth Rate Contributions

To illustrate the computational procedure, consider the first three irrotational terms:

$$\alpha_1 = \frac{1}{\exp(2\alpha_m t)E_m^2}\iiint_V \Bigg\langle -\nabla \cdot \left[\hat{p}\hat{\boldsymbol{u}} + \frac{1}{2}M_b U(\hat{p})^2\right]$$

$$- M_b[\hat{\boldsymbol{u}} \cdot \nabla(\boldsymbol{U} \cdot \hat{\boldsymbol{u}})]\Bigg\rangle\, dV \tag{36}$$

where the first two terms have been combined by using the vector identity for the divergence of the product of a scalar and a vector and by noting that $\nabla \cdot \boldsymbol{U} = 0$ for continuity of the incompressible mean flow. Thus, the first term can be converted to a surface integral using Gauss's divergence theorem. The second can be written in terms of the pressure by means of Eq. (33); after some algebra it also reduces to a surface integral. Assuming a short, quasi-steady nozzle, one finds

$$\alpha_1 = \frac{M_b}{2E_m^2}\left\{\iint_{S_b}\left[A_b^{(r)} + 1\right]\hat{p}_m^2\, dS - \iint_{S_N}\left[A_N^{(r)} + U_z\right]\hat{p}_m^2\, dS\right\}$$

$$\simeq \frac{\pi M_b}{2E_m^2}\frac{L}{R}\left\{\left[A_b^{(r)} + 1\right] - [\gamma + 1]\right\} \tag{37}$$

The first term in Eq. (37) is, of course, the classical pressure coupling effect, except that it is now somewhat reduced in size because of the larger energy normalization integral. The entire surface integral has not been represented in Eq. (37). Nonburning chamber surfaces can be accommodated in the surface integrals if required.

The several admittance functions are taken to be quantities of $\mathcal{O}(1)$; the mean flow Mach number has been factored out as in most traditional computations. The admittance for nonburning surfaces A_s is usually neglected, although rough chamber walls and insulation layers can display substantial (usually negative) admittance.

The fourth term, the volume (dilatational) acoustic viscous energy loss, is usually ignored in standard combustion stability computations; it is discussed extensively in the acoustic stability literature because it represents a main source of decay of acoustic waves in a variety of applications. It is readily evaluated for the present case with the result that

$$\alpha_2 = \frac{1}{E_m^2 \exp(2\alpha_m t)} \iiint_V \langle \delta_d^2 \hat{\boldsymbol{u}} \cdot \nabla(\nabla \cdot \hat{\boldsymbol{u}}) \rangle \, \mathrm{d}V \simeq -\frac{\delta_d^2 \pi k_m^2}{4 E_m^2} \frac{L}{R}$$

(38)

where Eq. (33) has again been used. Note that this damping effect might not be negligible when turbulence is present; then the transport properties are modified, and the effective viscosity coefficient might be much larger than the laminar values over a substantial volume of the chamber.[10] Other irrotational growth rate terms are not displayed here. These include effects of aluminum particulates and residual combustion.[76–78] Because the system is linear, they can be superposed later as required.

Two of the rotational terms are traditionally included with the strictly irrotational growth rate contributions just evaluated. These are the effects of the mean flow rotationality and the flow-turning effect. To account for the rotational mean flow, one writes

$$\alpha_3 = \frac{1}{E_m^2 \exp(2\alpha_m t)} \iiint_V \langle M_b[\hat{\boldsymbol{u}} \cdot (\hat{\boldsymbol{u}} \times \boldsymbol{\Omega})] \rangle \, \mathrm{d}V = \mathcal{O}(M_b^2) \quad (39)$$

as evaluated by Culick[2] in his rotational mean flow paper and shown by him to represent a negligible correction.

Before proceeding to the next term in Eq. (19), the reader is reminded that Culick first identified the flow-turning loss in his one-dimensional acoustic stability analysis.[4,47,79] As shown by Flandro,[8,9] this damping effect appears because, by requiring the unsteady flow to enter the duct in a direction perpendicular to the burning surface, Culick effectively invoked the no-slip condition. Although this term cannot arise in the multidimensional irrotational stability analysis, Culick insisted that it be "patched" onto the acoustic growth results. If we follow this dictum, we must add

$$\alpha_4 = \alpha_{\text{flow turning}} = \frac{E_m^{-2}}{\exp(2\alpha_m t)} \iiint_V \langle M_b \hat{\boldsymbol{u}} \cdot (\boldsymbol{U} \times \boldsymbol{\omega}) \rangle \, \mathrm{d}V$$

$$= \frac{-M_b E_m^{-2}}{k_m \exp(2\alpha_m t)} \iiint_V \langle \nabla \hat{p} \cdot (\boldsymbol{U} \times \boldsymbol{\omega}) \tan(k_m t) \rangle \, \mathrm{d}V$$

$$= \frac{-M_b E_m^{-2}}{k_m \exp(2\alpha_m t)} \iiint_V \langle \nabla \hat{p}_m \exp(\alpha_m t) \cdot (\boldsymbol{U} \times \boldsymbol{\omega}) \sin(k_m t) \rangle \, \mathrm{d}V$$

(40)

to the other irrotational terms. This is not justified in reality because the unsteady vorticity must be used in the evaluation of Eq. (40). Inclusion of this single rotational term in the energy balance to the exclusion of all of the others is a not a mathematically legitimate step. Nevertheless, we place it in Eq. (19) with the irrotational terms in accordance with accepted practice. In evaluating Eq. (40), it is necessary to remember that the unsteady vorticity is

$$\boldsymbol{\omega} = \nabla \times \tilde{\boldsymbol{u}} = \left(\frac{\partial \tilde{u}_r}{\partial z} - \frac{\partial \tilde{u}_z}{\partial r} \right) \boldsymbol{e}_\theta = -\frac{\partial \tilde{u}_z}{\partial r} \boldsymbol{e}_\theta + \mathcal{O}(M_b) \quad (41)$$

The derivative of the radial velocity component with respect to z is of the order of the mean Mach number and can therefore be dropped. Using Eq. (25) for the axial rotational velocity, the amplitude of the vorticity vector becomes

$$\omega = -\exp(\alpha_m t)\left[\frac{\partial \tilde{u}_m^{(r)}}{\partial r} \cos(k_m t) + \frac{\partial \tilde{u}_m^{(i)}}{\partial r} \sin(k_m t) \right] \quad (42)$$

Taking the cross product with the mean flow vector yields

$$\boldsymbol{U} \times \boldsymbol{\omega} = (-U_z \omega)\boldsymbol{e}_r + (U_r \omega)\boldsymbol{e}_z \quad (43)$$

For longitudinal modes the pressure gradient is in the z direction, so the flow-turning integral reduces to

$$\alpha_4 = -\frac{M_b}{2 E_m^2} \iiint_V U_r \frac{\partial \tilde{u}_m^{(i)}}{\partial r} \sin(k_m z) \, \mathrm{d}V \quad (44)$$

Flandro[8] showed that the volume integral of Eq. (44) can be reduced to a surface integral that is identical to Culick's original flow-turning expression (Secs. V.B and V.C of Ref. 8). Because the flow-turning integral is considered to be a key damping effect, it is appropriate to review its evaluation in detail for the axial mode case.

First, consider the derivative of the axial rotational velocity (the vorticity) appearing in Eq. (44):

$$\frac{\partial \tilde{u}_m^{(i)}}{\partial r} = -\sin x \exp\phi \frac{\partial(\cos\psi)}{\partial r} \sin(k_m z \sin x) + \cdots \quad (45)$$

Only the leading term in this derivative is shown because it is several orders of magnitude larger than the other terms resulting from chain-rule differentiation of factors such as $\sin x$ or $\exp\phi$. The reason for this expansion becomes obvious when it is remembered that the derivative of ψ with respect to r is proportional to the inverse of the mean flow Mach number as shown in Eq. (12). Then

$$\frac{\partial \tilde{u}_m^{(i)}}{\partial r} = \frac{k_m}{M_b U_r} \sin x \exp\phi \sin\psi \sin(k_m z \sin x) + \mathcal{O}(1) \quad (46)$$

and the volume integral of Eq. (44) can be evaluated for the assumed cylindrical chamber as

$$\alpha_4 = -\frac{1}{2} k_m E_m^{-2} \int_0^{2\pi} \mathrm{d}\theta \int_0^{L/R} \int_0^1 r \sin x \exp\phi \sin\psi$$

$$\times \sin(k_m z \sin x) \sin(k_m z) \, \mathrm{d}r \, \mathrm{d}z \quad (47)$$

To find the exact value, it is necessary to use numerical integration caused by the complicated radial dependence. Following the observation made in Ref. 8 (Sec. V.B) that the integrand oscillates around zero from the chamber axis to the surface, the value of the integral depends only on its behavior near the upper limit. Then to very good approximation

$$\alpha_4 = -\frac{\pi k_m}{E_m^2} \int_0^{L/R} \sin^2(k_m z) \, \mathrm{d}z \int_0^1 r \sin x \exp\phi \sin\psi \, \mathrm{d}r$$

$$= -\frac{\pi k_m}{2 E_m^2} \frac{L}{R} \int_0^1 r \sin x \exp\phi \sin\psi \, \mathrm{d}r \simeq -\frac{\pi M_b}{2 E_m^2} \frac{L}{R} \quad (48)$$

The final numerical value of this damping effect is the same as in Culick's original calculation if the acoustic form of the normalization parameter ($E_m^2 = \frac{1}{2}\pi L/R$) is inserted. Then $\alpha_4 = -M_b$ in dimensionless form, and the dimensional value becomes

$$\alpha_4^* = -M_b(a_0/R)\mathrm{s}^{-1} \quad (49)$$

C. Rotational Flow Correction

Consider now the first rotational flow stability integral in Eq. (19):

$$\alpha_5 = \frac{1}{E_m^2 \exp(2\alpha_m t)} \iiint_V \langle -\tilde{\boldsymbol{u}} \cdot \nabla \hat{p} \rangle \, \mathrm{d}V \quad (50)$$

A companion term, the product of the acoustic velocity with the pressure gradient term in the momentum equation, has already been evaluated and shown to give rise to the pressure coupling effect of central importance. The physical interpretation of Eq. (50) is apparent. It represents the rate of work done on the rotational part of the unsteady flow by the oscillatory pressure forces. In this respect it is analogous to the pressure coupling, which as already shown, collapses to a surface integral and is then interpreted as the $p \, \mathrm{d}V$ work done on the incoming flow.[1] Obviously, this term vanishes in

a strictly irrotational environment; hence, it does not appear in the usual acoustic stability computations. Using Eqs. (23) and (25) and carrying out the time averaging, Eq. (50) reduces to

$$\alpha_5 = -\frac{1}{2E_m^2} \iiint\limits_V \tilde{u}_m^{(r)} \cdot \nabla \hat{p}_m \, dV \qquad (51)$$

Notice that, for axial modes, it is only necessary to know the axial component of the rotational velocity field because the pressure gradient is in the z direction. No information regarding the rotational radial velocity is required in the evaluation of α_5. Equation (51) is readily evaluated for axial modes in a cylindrical chamber by the same method described for the flow-turning integral; one finds for low-order modes

$$\alpha_5 \simeq \frac{1}{2} \left(\pi M_b \big/ E_m^2 \right) (L/R) \qquad (52)$$

which is equal to the flow-turning result but opposite in sign.

The growth rate contribution α_5 has been the source of much dispute in the rocket combustion instability community (Brown, private communication). It must therefore be scrutinized here in full detail. It appears in Eq. (51) in its natural form as an integral over the chamber volume. When first reported,[8,9] α_5 arose as a surface integral because Culick's perturbed wave equation method was used for computing the growth rate. To display α_5 in its original format, convert Eq. (51) to surface integral form by application of Gauss's divergence theorem. Remembering that the rotational field is solenoidal, $\nabla \cdot \tilde{u} = 0$, and using the vector identity for the divergence of a scalar times a vector one can write

$$\nabla \cdot (\tilde{u}\hat{p}) = \tilde{u} \cdot \nabla \hat{p} + \hat{p} \nabla \cdot \tilde{u} = \tilde{u} \cdot \nabla \hat{p} \qquad (53)$$

The conversion to a surface integral follows immediately; one finds

$$\iiint\limits_V (\tilde{u} \cdot \nabla \hat{p}) \, dV = \iiint\limits_V \nabla \cdot (\tilde{u}\hat{p}) \, dV = \iint\limits_S (n \cdot \tilde{u}\hat{p}) \, dS \quad (54)$$

The growth rate contribution in surface integral form then becomes

$$\alpha_5 = -\frac{1}{2E_m^2} \iint\limits_S n \cdot \tilde{u}_m^{(r)} \hat{p}_m \, dS \qquad (55)$$

This is precisely the term described in Eq. (89) of Ref. 8 as the rotational flow correction, for want of a better name. The difficulty with the surface integral form is that its evaluation implies detailed knowledge of the normal component of the rotational velocity at the surface. This approach was followed in Refs. 8 and 9, and the radial component $n \cdot \tilde{u} = \tilde{u}_r$ was deduced by integrating the continuity equation.[11] It was found that the radial component of the rotational velocity $\tilde{u}_r$ is proportional to the mean flow Mach number, does not vanish at the edge of the combustion zone, and is proportional to the unsteady pressure mode shape.[8,9,11] These findings lead to an unfortunate interpretation, reported in Ref. 8, that α_5 can be treated as a correction to the surface coupling effect deduced in the irrotational part of the stability calculation. This forces one to search for new sources of mass flux within the flame zone. Critics (Brown, private communication) misinterpreted this observation to imply that changes in the surface response to pressure fluctuations are implied. The actual source of the new radial mass flux can be readily identified in the parallel gas motions within the combustion layer. Because there exists a momentum defect at the surface as a result of the no-slip requirement, additional oscillatory mass flux in the radial direction is generated. The simple control volume shown in Fig. 5 describes the two-dimensional field in the combustion zone and illustrates these ideas.

It is clear that, because of the gradient in axial velocity fluctuations parallel to the surface, there is a net flux of mass into the vertical sides of the control volume. This is reflected in the net unsteady mass flux at the edge of the combustion zone. It is this additional radial mass flux that is accounted for in Eq. (52); no modification of the oscillatory mass flux created by pressure coupling at the propellant side (i.e., solid/gas interface) of the control volume is implied.
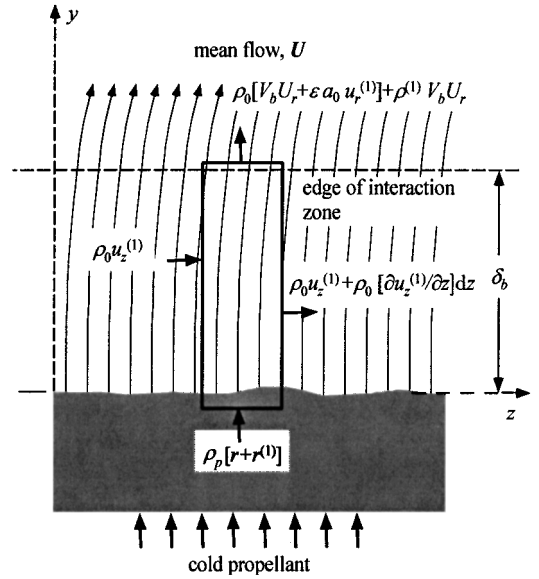

Fig. 5   Mass balance across the combustion zone.

The formal approach just described, carried out in detail, fully justifies the results reported in the earlier papers.[8,9] Despite these findings, the combustion instability community is understandably wary of any suggestion indicating that a mechanism other than the time-honored pressure coupling arises in the combustion zone. This point of confusion is partly resolved by using the volume integral form, Eq. (51), in place of the surface integral, Eq. (55). Both forms represent the same destabilizing influence on system stability, but the volume integral is more easily evaluated and is therefore the preferred form.

It is also important to understand that the rotational flow correction, Eq. (51), and the flow-turning integral, Eq. (51), are separate and distinct parts of the interaction of the acoustic field with vorticity production. Despite claims to the contrary, Eq. (51) is not an alternative way to represent flow turning. Brown has attempted to prove that the sign on α_5 given in Refs. 8 and 9 should be reversed (Brown, private communication). If he is correct in this assertion, then both contributions to the growth rate have the same sign. Because, as shown in Ref. 8, they have nearly equal magnitude, Brown then assumes that they must represent, in reality, the same physical effect. He claims that Eq. (51) duplicates what is already accounted for by Eq. (40). Because this assertion has resulted in confusion in the combustion stability research community, it is necessary to resolve the matter here.

Consider the combination of the flow turning and the rotational flow correction as represented by Eqs. (44) and (51). Their sum is

$$\alpha_4 + \alpha_5 = \frac{1}{2E_m^2} \iiint\limits_V \left[-M_b U_r \frac{\partial \tilde{u}_m^{(i)}}{\partial r} + k_m \tilde{u}_m^{(r)} \right] \sin(k_m z) \, dV \qquad (56)$$

If the value for the derivative of the imaginary part from Eq. (46) is used and Eq. (31) is substituted for the real part of the rotational axial velocity, then the integrand becomes

$$-M_b U_r \frac{\partial \tilde{u}_m^{(i)}}{\partial r} + k_m \tilde{u}_m^{(r)} = -M_b U_r \frac{k_m}{M_b U_r} \sin x \exp \phi \sin \psi$$

$$\times \sin(k_m z \sin x) + k_m \sin x \exp \phi \sin \psi \sin(k_m z \sin x) = 0 \qquad (57)$$

This proves that the flow turning is exactly canceled by the rotational flow correction as asserted in Refs. 8 and 9, that is,

$$\alpha_4 + \alpha_5 = 0 \qquad (58)$$

This result might seem contrary to some experimental results, which apparently require that flow turning be included for acceptable agreement with the stability theory.[80] Contrary opinions have been

expressed by many other experimentalists who find that removal of the flow turning leads to better agreement with motor growth rate data. However, several other rotational flow corrections remain to be evaluated. Let us reserve judgment until all of the pieces have been finally assembled.

D. More Rotational Growth Rate Contributions

It is now necessary to tackle the remaining terms in Eq. (19), a seemingly daunting task. None of these new terms has been accounted for in previous studies. Fortunately, some of them do not contribute significantly to the system energy balance. Again, it is instructive to examine these stability integrals individually.

The second term on the third line in Eq. (19) can be converted immediately to a surface integral by using standard vector identities and the fact that the rotational velocity field is solenoidal. One finds that

$$\iiint_V \langle -M_b \tilde{u} \cdot \nabla (U \cdot \hat{u}) \rangle \, \mathrm{d}V = \iint_S \langle -M_b n \cdot \tilde{u} (U \cdot \hat{u}) \rangle \, \mathrm{d}S$$
$$= \mathcal{O}(M_b^2) \qquad (59)$$

Because, as already shown, the normal velocity fluctuation at the surface is of order M_b, this term is negligible.

The third and fourth terms are most easily handled together. The volume integral can be converted to the sum of a surface integral and a simpler volume integral. The result is

$$\iiint_V \langle -M_b(\hat{u} + \tilde{u}) \cdot \nabla (U \cdot \tilde{u}) \rangle \, \mathrm{d}V = -M_b \iint_S \langle n \cdot u (U \cdot \tilde{u}) \rangle \, \mathrm{d}S$$
$$+ M_b \iiint_V \langle (U \cdot \tilde{u}) \nabla \cdot \hat{u} \rangle \, \mathrm{d}V \qquad (60)$$

where the surface integral is again second order in the Mach number because the normal velocity fluctuation is of the order of M_b. The surface integral can be expanded into

$$-M_b \iint_{S_N} \langle n \cdot u (U \cdot \tilde{u}) \rangle \, \mathrm{d}S = -M_b \iint_{S_N} \langle -(\hat{u}_z + \tilde{u}_z) U_z \tilde{u}_z \rangle \, \mathrm{d}S$$
$$= M_b \iint_{S_N} \langle \hat{u}_z U_z \tilde{u}_z \rangle \, \mathrm{d}S + M_b \iint_{S_N} \langle \tilde{u}_z U_z \tilde{u}_z \rangle \, \mathrm{d}S$$
$$= M_b \iint_{S_N} \langle \tilde{u}_z^2 U_z \rangle \, \mathrm{d}S \qquad (61)$$

Both steady and unsteady analytical expressions deteriorate in the proximity of the nozzle where the flow suddenly accelerates, becomes compressible, then choked at the throat. Evaluating the surface integral is further exacerbated by the open area and geometric irregularity associated with different motors. In view of these uncertainties, Eq. (61) has been routinely ignored.

The remaining volumetric integral in Eq. (60) must be evaluated. Using the continuity equation with Eq. (23), one writes

$$\nabla \cdot \tilde{u} = -\frac{\partial \hat{p}}{\partial t} = k_m \hat{p}_m \exp(\alpha_m t) \sin(k_m t) + \mathcal{O}(M_b) \qquad (62)$$

and inserting Eq. (25), one finds the growth rate to be

$$\frac{k_m M_b}{2E_m^2} \iiint_V \left[U \cdot \tilde{u}_m^{(i)} \right] \hat{p}_m \, \mathrm{d}V$$
$$= \frac{k_m M_b}{2E_m^2} \left\{ -2\pi^2 \int_0^1 \cos x \sin x \exp \phi \cos \psi \right.$$
$$\left. \times \left[\int_0^{L/R} z \sin(k_m z \sin x) \, \mathrm{d}z \right] \mathrm{d}r \right\} \qquad (63)$$

The radial integral yields a value of the order of the mean Mach number, and so this term represents a negligible growth rate contribution.

The fifth term is highly interesting because it is the companion of the original flow-turning effect represented by Eq. (40). Now, we must evaluate

$$\alpha_6 = \frac{1}{E_m^2 \exp(2\alpha_m t)} \iiint_V \langle M_b \tilde{u} \cdot (U \times \omega) \rangle \, \mathrm{d}V \qquad (64)$$

where the rotational velocity appears in the place of the acoustic velocity as in the flow-turning integral. Using Eq. (42) for the unsteady vorticity and dropping terms of the second order, one finds

$$\alpha_6 = -\frac{M_b}{4E_m^2} \iiint_V U_r \frac{\partial}{\partial r} \left[\tilde{u}^{(r)} \cdot \tilde{u}^{(r)} + \tilde{u}^{(i)} \cdot \tilde{u}^{(i)} \right] \mathrm{d}V \qquad (65)$$

Inserting the expressions for the rotational velocity and integrating over the volume, one finds, for a cylindrical chamber,

$$\alpha_6 = \frac{\pi M_b}{4E_m^2} \frac{L}{R} \int_0^1 \sin x \frac{\partial}{\partial r} \sin^2 x \exp^2 \phi \, \mathrm{d}r \simeq \frac{\pi M_b}{4E_m^2} \frac{L}{R} \qquad (66)$$

This is an energy source rather than a sink, as was the case for the flow turning. In a sense it represents an unexpected finding. Conventional analyses indicate that the only energy source in the motor chamber is that produced by the pressure coupled combustion response; all other stability integrals are thought to be sinks of energy. This new source term is clearly related to the creation of unsteady vorticity at the boundaries, even when viscosity is discounted. For this reason, α_6 will be referred to as the inviscid vortical correction. Notice that α_6 has been evaluated here only for the vorticity produced at the surface as a natural consequence of the no-slip condition in the case of the axial acoustic mode. If, for example, one takes account of vortex shedding effects [including the parietal vortex shedding mechanism (PVS)], this term must be evaluated with appropriate modifications to the vorticity vector and rotational unsteady flow. Additional contributions to system instability from α_6 must then be expected. Future work will be focused on these potentially important interactions.

The sixth remaining term involves the volume integral

$$\iiint_V -M_b \langle -\tilde{u} \cdot (\hat{u} \times \Omega) \rangle \, \mathrm{d}V \qquad (67)$$

This growth rate contribution is negligible because the cross product yields an axial vector component proportional to the radial acoustic velocity. Therefore, only terms of second order in the mean flow Mach number are generated.

The last two terms are viscous damping expressions. In the classical (irrotational) combustion instability calculations viscous effects are ignored completely on the basis that there are no strong velocity gradients at the surface to give rise to significant shearing stresses. Acoustic boundary-layer corrections of the usual sort do not properly account for the shearing stresses when there is strong convection through the surface layer. A correction to the dilatational (volume damping) effect is represented in the seventh rotational term. Using the same methods used to evaluate the other terms, this one can be transformed into a surface integral, namely,

$$\iiint_V \left\langle \delta_d^2 \tilde{u} \cdot \nabla (\nabla \cdot \hat{u}) \right\rangle \mathrm{d}V = -\delta_d^2 \iint_S \left\langle n \cdot \tilde{u} \frac{\partial p^{(1)}}{\partial t} \right\rangle \mathrm{d}S \qquad (68)$$

which, for realistic values of the parameters, must be negligible because both the dimensionless viscosity coefficient δ_d^2 and the normal velocity at the bounding surfaces are of the order of the mean flow Mach number.

Finally, the last term represents the viscous damping

$$\alpha_7 = \frac{1}{E_m^2 \exp(2\alpha_m t)} \iiint_V \langle -\delta^2 (\hat{u} + \tilde{u}) \cdot (\nabla \times \omega) \rangle \, \mathrm{d}V \qquad (69)$$

where the composite unsteady velocity appears instead of just the acoustic part as in previous works [see Eq. (95) in Ref. 8]. After carrying out the indicated calculations and inserting the various

components of the velocity vectors, the viscous growth rate reduces to

$$
\alpha_7 = \frac{\delta^2}{2E_m^2} \iiint_V \left[\tilde{u}_m^{(r)} \frac{\partial^2 \tilde{u}_m^{(r)}}{\partial r^2} + \tilde{u}_m^{(i)} \frac{\partial^2 \tilde{u}_m^{(i)}}{\partial r^2} \right] dV
$$

$$
= -\frac{\delta^2}{2E_m^2} \left(\frac{k_m}{M_b}\right)^2 \iiint_V r^2 \exp^2 \phi \sin^2(k_m z)\, dV \qquad (70)
$$

where smaller terms have been dropped. This expression is easily evaluated for a full-length cylindrical grain. The result is

$$
\alpha_7 \simeq -\frac{\pi \delta^2}{6E_m^2} \frac{L}{R} \left(\frac{k_m}{M_b}\right)^2 = -\frac{\pi M_b \xi}{6E_m^2} \frac{L}{R} \qquad (71)
$$

to good approximation. Notice that the importance of viscous damping increases rapidly with frequency. Because the square of the Mach number appears in the denominator, this term can be as important as any of the others retained in the analysis. Contrary to earlier assessments, we find that viscous damping must not be discarded, especially in the case of turbulent mean flows. Then the transport properties are modified, and δ^2 might be much larger than for the laminar case. To evaluate Eq. (70) properly in the turbulent case, a comprehensive numerical algorithm will be needed. Work of this sort has already begun.[10,18,19]

E. Pseudopressure Growth Rate Corrections

The last two terms in Eq. (19) are caused by interactions between the unsteady velocity field and the pseudopressure associated with the vorticity-driven disturbances. These two terms need to be carefully evaluated from

$$
\alpha_8 = \frac{-1}{E_m^2 \exp(2\alpha_m t)} \iiint_V \langle \hat{\boldsymbol{u}} \cdot \nabla \tilde{p} \rangle\, dV \qquad (72)
$$

$$
\alpha_9 = \frac{-1}{E_m^2 \exp(2\alpha_m t)} \iiint_V \langle \tilde{\boldsymbol{u}} \cdot \nabla \tilde{p} \rangle\, dV \qquad (73)
$$

Using Eq. (9), one finds

$$
\alpha_8 = \frac{-\pi M_b}{4E_m^2} \iiint_V \sin(k_m z)\ \sin(2x) \exp(\phi) \cos(\psi)
$$

$$
\times \{\sin[k_m z \sin(x)] + k_m z\ \sin(x) \cos[k_m z \sin(x)]\}\, dV
$$

$$
\simeq \frac{M_b^3}{E_m^2 k_m^2} \frac{L}{R} \qquad (74)
$$

Clearly, α_8 is small, being of order M_b^3. The remaining pseudorotational correction needs to be evaluated from

$$
\alpha_9 = \frac{\pi M_b}{4E_m^2} \iiint_V \big(\sin(2x) \sin(x) \exp(2\phi)\{\sin[k_m z \sin(x)]
$$

$$
+ k_m z \sin(x) \cos[k_m z \sin(x)]\} \sin[k_m z \sin(x)]
$$

$$
+ k_m z \sin^2(x) \sin(2x) \exp(2\phi) \sin[k_m z \sin(x)]
$$

$$
\times \cos[k_m z \sin(x)]\big)\, dV \simeq \frac{9\pi^2 M_b}{200 E_m^2} \frac{L}{R} \qquad (75)
$$

Unlike α_8, α_9 is of the same order as α_6; this new term constitutes another destabilizing source that needs to be retained.

III. Discussion

The system stability is determined by superposition of a set of stability integrals that includes both the original set found from the classical irrotational analysis and several new ones that represent the effects of the rotational unsteady flow. We must now assess the impact of the proposed changes on stability assessment methodology.

It is useful to compare the theoretical irrotational and rotational calculations for typical motor parameters. Please note that account is not taken of other gain loss effects such as particulate drag and residual combustion that could be important in real rocket motors. Then for the classical model the growth rate is

$$
\alpha_{\text{standard}} = \alpha_1 + \alpha_2 + \alpha_3 + \alpha_4 \qquad (76)
$$

which includes the flow-turning correction that is usually assumed and where evaluations are to be made using the irrotational energy normalization value

$$
\left(E_m^2\right)_{\text{standard}} = \tfrac{1}{2}\pi L/R \qquad (77)
$$

for the case of axial modes in a cylindrical combustion chamber.

For the new stability calculation, including additional rotational corrections, one must use

$$
\alpha_{\text{composite}} = \alpha_1 + \alpha_2 + \alpha_3 + \alpha_6 + \alpha_7 + \alpha_8 + \alpha_9 \qquad (78)
$$

where the cancellation of the flow-turning effect and the rotational flow correction is accounted for; furthermore, evaluations must be made using the corrected energy normalization value

$$
\left(E_m^2\right)_{\text{composite}} = \tfrac{5}{8}\pi L/R \qquad (79)
$$

written, again, for axial modes in a full-length cylinder.

No attempt is made here to compare numerical values to experimental results published recently, which come from nonlinear decay data.[80,81] It has been claimed that some measurements demonstrate that the standard acoustic stability results give acceptable prediction of the observed behavior. It must be remarked that none of the experimental points illustrated are taken from sections of the data where there was rapid growth in the waves; only pulse decay data were utilized. The standard stability calculations did not predict linear growth for any of the motors tested. Careful study of the data reduction process suggests that the reason data points displayed show unusually high damping is that it was necessary to filter the data to eliminate the strong harmonic content; the presence of higher modes with quite appreciable amplitude accompanying the filtered first mode data indicates nonlinear interactions that cannot be ignored. Linear theory does not apply in the situation described.[80,81]

A few simple calculations will demonstrate some features of the results found here. It is quite easy to apply the formulas for a cylindrical chamber. Table 1 from Ref. 9, showing values for the key parameters for representative motors, is reproduced here for convenience. Let us focus on large motors of the type described as SRB in the table. As described in the Introduction, there have been many observations of longitudinal mode instability in large motors such as the SRB. These oscillations have most often been attributed to vortex shedding phenomena. In that model the natural instability of the mean flow, especially when flow separation is present, suggests that large-scale vortex structures are generated, which can add energy to the unsteady field in the manner of a wind musical instrument.

Let us test the result of the analysis given here by applying it to a simplified SRB geometry in which the grain is assumed to be a long, straight, and unsegmented cylinder. No measurements of the propellant admittance function need to be attempted for the SRB

Table 1   Physical parameters for typical motor systems

Motor	L, m	R, m	M_b	δ	k_m	S	ξ	$A_b^{(r)}$	f, Hz
Small motor (Yang and Culick)	0.60	0.025	1.7^{-3}	5.49^{-4}	1.33^{-1}	76.87	1.0309	2.5	1227
Tactical rocket (Typical geometry)	2.03	0.102	3.1^{-3}	2.74^{-4}	1.58^{-1}	50.84	0.0624	1.2	360
Space shuttle SRB	35.1	0.700	2.3^{-3}	1.04^{-4}	6.27^{-2}	27.24	0.0035	1.0	19.5

Table 2 Comparison of stability estimates

Motor	$A_b^{(r)}$	f, Hz	α_{standard}, s^{-1}	$\alpha_{\text{composite}}$, s^{-1}
Small motor (Yang and Culick)	2.50	1227	20.0	131
Tactical rocket (Typical geometry)	1.20	360	−48.9	23.5
Space shuttle SRB	1.00	19.5	−5.85	1.73

propellant because the natural frequencies in this long motor are low (19.5-Hz first mode, notwithstanding the effect of end cavities). Hence, one can assume a typical (dimensionless) value of $A_b^{(r)} \simeq 1$ for this situation. Standard short nozzle damping is also assumed. No attempt is made to account for particle damping because this effect is negligible for such a low frequency of oscillation. Application of the standard stability code yields, for this case,

$$\alpha_{\text{standard}} \simeq -5.85 \text{ s}^{-1} \qquad (80)$$

Being comparable to values that were computed during the development of this motor standard predictions lead to the impression that the SRB would be very stable. For such large motors growth or decay rates are always found to be small. The result is misleading because, in practice, significant thrust oscillations (∼20 klbf peak to peak) are observed in static tests of all versions of the SRBs. Oscillations are also detected in flight with amplitudes sometimes exceeding 2 psi (peak to peak). If the new analysis is used instead, one finds

$$\alpha_{\text{composite}} \simeq 1.73 \text{ s}^{-1} \qquad (81)$$

The new result reconciles with actual observations indicating that strong vorticity waves should be expected in this motor. It is interesting that the growth rate predictions for the next two or three longitudinal modes are of the same order of magnitude as the first mode results shown. In the SRB case three or four modes were always readily discernible in the waterfall data.

Table 2 shows comparisons of stability results (first axial acoustic mode) for three of the configurations defined in Table 1. Typical admittance values are used, and particulate damping and other two-phase flow effects are ignored. In all cases, the new model predicts a less stable system. This is due mainly to the effective cancellation of the flow-turning damping term. This greatly improves agreement between theory and experiment as demonstrated in Ref. 8. In larger motors (e.g., Shuttle SRB), the new term α_6 also introduces a significant change in system stability. The new results predict unstable behavior in agreement with much experimental data. The original SSPP calculations indicated that the Shuttle and Ariane motors (and similar large solid rocket boosters) were not susceptible to oscillatory waves.

IV. Conclusions

The new stability estimation method described in this paper displays new energy source terms not found in the acoustic instability methodology. The new results help to explain the growth of longitudinal oscillations in large solid-propellant motors that have appeared in many development programs. Considerable work lies ahead in fully utilizing what we have found as the basis for a predictive algorithm for use in motor design and in data reduction and interpretation. Although the general formulation is not geometry dependent, we have relied heavily on the assumption of a simple cylindrical geometry with longitudinal plane wave oscillations to enable the evaluations shown.

Clearly much work will be needed to determine the stability characteristics of waves in more realistic motor configurations. Extension of the results to partial grains requires further study. Complex geometrical features of the burning port such as slots and fins represent difficulties that might require a full numerical treatment of both the steady and the unsteady flow by application of computational fluid dynamics. Inclusion of regions of separated flow, for example, at segment interfaces in large motors, introduces additional complications. Full Navier–Stokes solutions might eventually provide

the necessary information. It is possible that new numerical simulations can be validated by use of the analytical models that have been described herein.

The new results introduced in this paper can be readily tested using an experimental apparatus already in place. For instance, the cold flow models used by French investigators in their Ariane work could be used to test the new theoretical framework. Because only growth rates are predicted in the linearized theory, it would be necessary to modify the test procedure in such a way that transient behavior could be assessed.

In the latter regard new emphasis on modeling of the nonlinear aspects of unsteady flow with rotational flow corrections is clearly justified. There are no methods available for predicting important features of real motor operation such as limit-cycle amplitude or triggering. Certainly, rotational flow effects will play a central role in resolving these difficulties.

Finally, new stability integrals discovered in the present work, in particular, the inviscid vortical growth rate α_6 and the pseudo-pressure-rotational growth rate α_9, might have a bearing on the unresolved problem of velocity coupling. Both growth rate terms represent distinct avenues by which velocity fluctuations $\tilde{u}$ affect the system stability. In fact, the inviscid vortical term α_6 can be recast in the form of a surface integral, and it is then obvious that a "velocity coupling" response function can be connected to it. These matters require further study.

References

[1]Culick, F. E. C., "Acoustic Oscillations in Solid Propellant Rocket Chambers," *Acta Astronautica*, Vol. 12, No. 2, 1966, pp. 113–126.

[2]Culick, F. E. C., "Rotational Axisymmetric Mean Flow and Damping of Acoustic Waves in a Solid Propellant Rocket," *AIAA Journal*, Vol. 4, No. 8, 1966, pp. 1462–1464.

[3]Culick, F. E. C., "Stability of Longitudinal Oscillations with Pressure and Velocity Coupling in a Solid Propellant Rocket," *Combustion Science and Technology*, Vol. 2, No. 4, 1970, pp. 179–201.

[4]Culick, F. E. C., "The Stability of One-Dimensional Motions in a Rocket Motor," *Combustion Science and Technology*, Vol. 7, No. 4, 1973, pp. 165–175.

[5]Culick, F. E. C., "Stability of Three-Dimensional Motions in a Rocket Motor," *Combustion Science and Technology*, Vol. 10, No. 3, 1974, pp. 109–124.

[6]Lovine, R. L., Dudley, D. P., and Waugh, R. D., "Standardized Stability Prediction Method for Solid Rocket Motors," Vols. 1, 2, and 3, Aerojet Solid Propulsion Co., Rept. AFRPL TR 76-32, San Jose, CA, May 1976.

[7]Nickerson, G. R., Culick, F. E. C., and Dang, L. G., "Standardized Stability Prediction Method for Solid Rocket Motors Axial Mode Computer Program," Software and Engineering Associates, Inc., AFRPL TR-83-017, San Jose, CA, Sept. 1983.

[8]Flandro, G. A., "Effects of Vorticity on Rocket Combustion Stability," *Journal of Propulsion and Power*, Vol. 11, No. 4, 1995, pp. 607–625.

[9]Flandro, G. A., "On Flow Turning," AIAA Paper 95-2530, July 1995.

[10]Flandro, G. A., Cai, W., and Yang, V., "Turbulent Transport in Rocket Motor Unsteady Flowfield," *Solid Propellant Chemistry, Combustion, and Motor Interior Ballistics*, edited by V. Yang, T. B. Brill, and W.-Z. Ren, Vol. 185, Progress in Astronautics and Aeronautics, AIAA, Reston, VA, 2000, pp. 837–858.

[11]Majdalani, J., Flandro, G. A., and Roh, T. S., "Convergence of Two Flowfield Models Predicting a Destabilizing Agent in Rocket Combustion," *Journal of Propulsion and Power*, Vol. 16, No. 3, 2000, pp. 492–497.

[12]Majdalani, J., and Van Moorhem, W. K., "Improved Time-Dependent Flowfield Solution for Solid Rocket Motors," *AIAA Journal*, Vol. 36, No. 2, 1998, pp. 241–248.

[13]Majdalani, J., "Boundary-Layer Structure in Cylindrical Rocket Motors," *AIAA Journal*, Vol. 37, No. 4, 1999, pp. 505–508.

[14]Majdalani, J., "Vorticity Dynamics in Isobarically Closed Porous Channels. Part 1: Standard Perturbations," *Journal of Propulsion and Power*, Vol. 17, No. 2, 2001, pp. 355–362.

[15]Majdalani, J., and Roh, T. S., "Vorticity Dynamics in Isobarically Closed Porous Channels. Part 2: Space-Reductive Perturbations," *Journal of Propulsion and Power*, Vol. 17, No. 2, 2001, pp. 363–370.

[16]Majdalani, J., and Roh, T. S., "The Oscillatory Channel Flow with Large Wall Injection," *Proceedings of the Royal Society, Series A*, Vol. 456, No. 1999, 2000, pp. 1625–1657.

[17]Vuillot, F., and Avalon, G., "Acoustic Boundary Layer in Large Solid Propellant Rocket Motors Using Navier–Stokes Equations," *Journal of Propulsion and Power*, Vol. 7, No. 2, 1991, pp. 231–239.

[18]Roh, T. S., Tseng, I. S., and Yang, V., "Effects of Acoustic Oscillations on Flame Dynamics of Homogeneous Propellants in Rocket Motors," *Journal of Propulsion and Power*, Vol. 11, No. 4, 1995, pp. 640–650.

[19]Yang, V., and Roh, T. S., "Transient Combustion Response of Solid Propellant to Acoustic Disturbance in Rocket Motors," AIAA Paper 95-0602, Jan. 1995.

[20]Vuillot, F., "Numerical Computation of Acoustic Boundary Layers in Large Solid Propellant Space Booster," AIAA Paper 91-0206, Jan. 1991.

[21]Baum, J. D., Levine, J. N., and Lovine, R. L., "Pulsed Instabilities in Rocket Motors: A Comparison Between Predictions and Experiments," *Journal of Propulsion and Power*, Vol. 4, No. 4, 1988, pp. 308–316.

[22]Baum, J. D., "Investigation of Flow Turning Phenomenon; Effects of Frequency and Blowing Rate," AIAA Paper 89-0297, Jan. 1989.

[23]Glick, R. L., and Renie, J. P., "On the Nonsteady Flowfield in Solid Rocket Motors," AIAA Paper 84-1475, June 1984.

[24]Brown, R. S., Blackner, A. M., Willoughby, P. G., and Dunlap, R., "Coupling Between Acoustic Velocity Oscillations and Solid Propellant Combustion," *Journal of Propulsion and Power*, Vol. 2, No. 5, 1986, pp. 428–437.

[25]Shaeffer, C. W., and Brown, R. S., "Oscillatory Internal Flow Field Studies," United Technologies, AFOSR CR F04620-90-C-0032, San Jose, CA, 1990.

[26]Shaeffer, C. W., and Brown, R. S., "Oscillatory Internal Flow Studies," Chemical Systems Div., TR 2060 FR, United Technologies, San Jose, CA, Aug. 1992.

[27]Cantrell, R. H., and Hart, R. W., "Interaction Between Sound and Flow in Acoustic Cavities: Mass, Momentum, and Energy Considerations," *Journal of the Acoustical Society of America*, Vol. 36, No. 4, 1964, pp. 697–706.

[28]Avalon, G., Casalis, G., and Griffond, J., "Flow Instabilities and Acoustic Resonance of Channels with Wall Injection," AIAA Paper 98-3218, July 1998.

[29]Lupoglazoff, N., and Vuillot, F., "Numerical Simulations of Parietal Vortex-Shedding Phenomenon in a Cold-Flow Set-Up," AIAA Paper 98-3220, July 1998.

[30]Lupoglazoff, N., and Vuillot, F., "Parietal Vortex Shedding as a Cause of Instability for Long Solid Propellant Motors. Numerical Simulations and Comparisons with Firing Tests," AIAA Paper 96-0761, Jan. 1996.

[31]Lupoglazoff, N., and Vuillot, F., "Numerical Simulation of Vortex Shedding Phenomenon in Two-Dimensional Test Case Solid Rocket Motors," AIAA Paper 92-0776, Jan. 1992.

[32]Prevost, M., Vuillot, F., and Traineau, J. C., "Vortex-Shedding Driven Oscillations in Subscale Motors for the Ariane 5 MPS Solid Rocket Motors," AIAA Paper 96-3247, July 1996.

[33]Scippa, S., Pascal, P., and Zanier, F., "Ariane 5 MPS -Chamber Pressure Oscillations Full Scale Firings Results Analysis and Further Studies," AIAA Paper 94-3068, June 1994.

[34]Fukushima, Y., "H-Ii Launcher Propulsion Experience," 5th AAAF Symposium International on Propulsion in Space Transportation, AAAF Paper 5.9-5.20, May 1996.

[35]Brown, R. S., Dunlap, R., Young, S. W., and Waugh, R. C., "Vortex Shedding as a Source of Acoustic Energy in Segmented Solid Rockets," *Journal of Spacecraft and Rockets*, Vol. 18, No. 4, 1981, pp. 312–319.

[36]Dotson, K. W., Koshigoe, S., and Pace, K. K., "Vortex Shedding in a Large Solid Rocket Motor Without Inhibitors at the Segment Interfaces," *Journal of Propulsion and Power*, Vol. 13, No. 2, 1997, pp. 197–206.

[37]Dotson, K. W., Murdock, J. W., and Kamimoto, D. K., "Launch Vehicle Dynamic and Control Effects from Solid Rocket Motor Slag Ejection," *Journal of Propulsion and Power*, Vol. 15, No. 3, 1999, pp. 468–475.

[38]Dotson, K. W., Baker, R. L., and Sako, B. H., "Launch Vehicle Self-Sustained Oscillation from Aeroelastic Coupling Part 1: Theory," *Journal of Spacecraft and Rockets*, Vol. 35, No. 3, 1998, pp. 365–373.

[39]Dotson, K. W., Baker, R. L., and Bywater, R. J., "Launch Vehicle Self-Sustained Oscillation from Aeroelastic Coupling Part 2: Analysis," *Journal of Spacecraft and Rockets*, Vol. 35, No. 3, 1998, pp. 374–379.

[40]Nesman, T., "RSRM Chamber Pressure Oscillations: Full Scale Ground and Flight Test Summary and Air Flow Test Results," 31st AIAA Joint Propulsion Conf., AIAA Solid Rocket Technical Committee, July 1995, pp. 27–48.

[41]Hart, R. W., and McClure, F. T., "Combustion Instability: Acoustic Interaction with a Burning Propellant Surface," *Journal of Chemical Physics*, Vol. 10, No. 6, 1959, pp. 1501–1514.

[42]Hart, R. W., Bird, J. F., Cantrell, R. H., and McClure, F. T., "Nonlinear Effects in Instability of Solid Propellant Rocket Motors," *AIAA Journal*, Vol. 2, No. 7, 1964, pp. 1270–1273.

[43]Hart, R. W., and McClure, F. T., "Theory of Acoustic Instability in Solid Propellant Rocket Combustion," *Tenth Symposium (International) on Combustion*, 1964, pp. 1047–1066.

[44]Culick, F. E. C., "Non-Linear Growth and Limiting Amplitude of Acoustic Oscillations in Combustion Chambers," *Combustion Science and Technology*, Vol. 3, No. 1, 1971, pp. 1–16.

[45]Culick, F. E. C., Burnely, V. S., and Swenson, G., "Pulsed Instabilities in Solid-Propellant Rockets," *Journal of Propulsion and Power*, Vol. 11, No. 4, 1995, pp. 657–665.

[46]Culick, F. E. C., "Some Recent Results for Nonlinear Acoustics in Combustion Chambers," *AIAA Journal*, Vol. 32, No. 1, 1994, pp. 146–168.

[47]Culick, F. E. C., and Yang, V., "Prediction of the Stability of Unsteady Motions in Solid Propellant Rocket Motors," *Nonsteady Burning and Combustion Stability of Solid Propellants*, edited by L. De Luca, E. W. Price, and M. Summerfield, Vol. 143, Progress in Astronautics and Aeronautics, AIAA, Washington, DC, 1992, pp. 719–779.

[48]Culick, F. E. C., "Rotational Axisymmetric Mean Flow and Damping of Acoustic Waves in a Solid Propellant Rocket," *Journal of Propulsion and Power*, Vol. 5, No. 6, 1989, pp. 657–664.

[49]Avalon, G., and Comas, P., "Simulative Study of the Unsteady Flow Inside a Solid Propellant Rocket Motor," AIAA Paper 91-1866, June 1991.

[50]Vuillot, F., "Vortex-Shedding Phenomena in Solid Rocket Motors," *Journal of Propulsion and Power*, Vol. 11, No. 4, 1995, pp. 626–639.

[51]Traineau, J. C., Prevost, M., and Lupoglazoff, N., "A Subscale Test Program to Assess the Vortex Shedding Driven Instabilities in Segmented Solid Rocket Motors," AIAA Paper 97-3247, July 1997.

[52]Vuillot, F., Traineau, J. C., Prevost, M., and Lupoglazoff, N., "Experimental Validation of Stability Assessment Methods for Segmented Solid Propellant Motors," AIAA Paper 93-1883, Jan. 1993.

[53]Couton, D., Doan-Kim, S., and Vuillot, F., "Numerical Simulation of Vortex-Shedding Phenomenon in a Channel with Flow Induced Through Porous Wall," *International Journal of Heat and Fluid Flow*, Vol. 18, No. 3, 1997, pp. 283–296.

[54]Tissier, P. Y., Godfroy, F., and Jacquemin, P., "CFD Analysis of Vortex Shedding Inside a Subscale Segmented Motor," AIAA Paper 94-2781, June 1994.

[55]Tissier, P. Y., Godfroy, F., and Jacquemin, P., "Simulation of Three Dimensional Flows Inside Solid Propellant Rocket Motors Using a Second Order Finite Volume Method—Application to the Study of Unstable Phenomena," AIAA Paper 92-3275, July 1992.

[56]Traineau, J. C., Hervat, P., and Kuentzmann, P., "Cold-Flow Simulation of a Two-Dimensional Nozzleless Solid-Rocket Motor," AIAA Paper 86-1447, July 1986.

[57]Vuillot, F., and Lupoglazoff, N., "Combustion and Turbulent Flow Effects in 2-D Unsteady Navier–Stokes Simulations of Oscillatory Rocket Motors," AIAA Paper 96-0884, Jan. 1996.

[58]Vuillot, F., Dupays, J., Lupoglazoff, N., Basset, T., and Daniel, E., "2-D Navier–Stokes Stability Computations for Solid Rocket Motors: Rotational, Combustion and Two-Phase Flow Effects," AIAA Paper 97-3326, July 1997.

[59]Ugurtas, B., Avalon, G., Lupoglazoff, N., and Vuillot, F., "Numerical Computations of Hydrodynamic Instabilities Inside Channels with Wall Injection," AIAA Paper 99-2505, June 1999.

[60]Casalis, G., Avalon, G., and Pineau, J.-P., "Spatial Instability of Planar Channel Flow with Fluid Injection Through Porous Walls," *Physics of Fluids*, Vol. 10, No. 10, 1998, pp. 2558–2568.

[61]Griffond, J., Casalis, G., and Pineau, J.-P., "Spatial Instability of Flow in a Semiinfinite Cylinder with Fluid Injection Through Its Porous Walls," *European Journal of Mechanics B/Fluids*, Vol. 19, No. 1, 2000, pp. 69–87.

[62]Griffond, J., and Casalis, G., "On the Dependence on the Formulation of Some Nonparallel Stability Approaches Applied to the Taylor Flow," *Physics of Fluids*, Vol. 12, No. 2, 2000, pp. 466–468.

[63]Griffond, J., and Casalis, G., "On the Nonparallel Stability of the Injection Induced Two-Dimensional Taylor Flow," *Physics of Fluids*, Vol. 13, No. 6, 2001, pp. 1635–1644.

[64]Varapaev, V. N., and Yagodkin, V. I., "Flow Stability in a Channel with Porous Walls," *Fluid Dynamics*, Vol. 4, No. 5, 1969, pp. 91–95.

[65]Ugurtas, B., Avalon, G., Lupoglazoff, N., Vuillot, F., and Casalis, G., "Stability and Acoustic Resonance of Internal Flows Generated by Side Injection," *Solid Propellant Chemistry, Combustion, and Motor Interior Ballistics*, edited by V. Yang, T. B. Brill, and W.-Z. Ren, Vol. 185, Progress in Astronautics and Aeronautics, AIAA, Reston, VA, 2000, pp. 823–836.

[66]Chu, B.-T., and Kovásznay, L. S. G., "Non-Linear Interactions in a Viscous Heat-Conducting Compressible Gas," *Journal of Fluid Mechanics*, Vol. 3, No. 5, 1957, pp. 494–514.

[67]Morse, P. M., and Ingard, K. U., *Theoretical Acoustics*, McGraw–Hill, New York, 1968, pp. 278, 279.

[68]Barron, J., Majdalani, J., and Van Moorhem, W. K., "A Novel Investigation of the Oscillatory Field over a Transpiring Surface," *Journal of Sound and Vibration*, Vol. 235, No. 2, 2000, pp. 281–297.

[69]Brown, R. S., Blackner, A. M., Willoughby, P. G., and Dunlap, R., "Coupling Between Velocity Oscillations and Solid Propellant Combustion," AIAA Paper 86-0531, Jan., 1986.

[70]Majdalani, J., and Van Moorhem, W. K., "Laminar Cold-Flow Model for the Internal Gas Dynamics of a Slab Rocket Motor," *Journal of Aerospace Science and Technology*, Vol. 5, No. 3, 2001, pp. 193–207.

[71]Majdalani, J., "Vortical and Acoustical Mode Coupling Inside a Two-Dimensional Cavity with Transpiring Walls," *Journal of the Acoustical Society of America*, Vol. 106, No. 1, 1999, pp. 46–56.

[72]Kirchoff, G., *Vorlesungen Über Mathematische Physik: Mechanik*, 2nd ed., Teubner, Leibzig, 1877, pp. 311–336.

[73]Apte, S., and Yang, V., "Effects of Acoustic Oscillations on Turbulent Flowfield in a Porous Chamber with Surface Transpiration," AIAA Paper 98-3219, July 1998.

[74]Beddini, R. A., and Roberts, T. A., "Turbularization of an Acoustic Boundary Layer on a Transpiring Surface," *AIAA Journal*, Vol. 26, No. 8, 1988, pp. 917–923.

[75]Beddini, R. A., and Roberts, T. A., "Response of Propellant Combustion to a Turbulent Acoustic Boundary Layer," *Journal of Propulsion and Power*, Vol. 8, No. 2, 1992, pp. 290–296.

[76]Thomas, H. D., Flandro, G. A., and Flanagan, S. N., "Effects of Vorticity on Particle Damping," AIAA Paper 95-2736, July 1995.

[77]Dupays, J., Prevost, M., Tarrin, P., and Vuillot, F., "Effects of Particulate Phase on Vortex Shedding Driven Oscillations in Solid Rocket Motors," AIAA Paper 96-3248, July 1996.

[78]Sabnis, J. S., de Jong, F. J., and Gibeling, H. J., "Calculation of Particle Trajectories in Solid-Rocket Motors with Arbitrary Acceleration," *Journal of Propulsion and Power*, Vol. 8, No. 5, 1992, pp. 961–967.

[79]Culick, F. E. C., "Remarks on Entropy Production in the One-Dimensional Approximation to Unsteady Flow in Combustion Chambers," *Combustion Science and Technology*, Vol. 15, No. 4, 1977, pp. 93–97.

[80]Blomshield, F. S., Crump, J. E., Mathes, H. B., Stalnaker, R. A., and Beckstead, M. W., "Stability Testing of Full-Scale Tactical Motors," *Journal of Propulsion and Power*, Vol. 13, No. 3, 1997, pp. 349–355.

[81]Blomshield, F. S., Mathes, H. B., Crump, J. E., Beiter, C. A., and Beckstead, M. W., "Nonlinear Stability Testing of Full-Scale Tactical Motors," *Journal of Propulsion and Power*, Vol. 13, No. 3, 1997, pp. 356–366.

J. P. Gore
Associate Editor